THE ARCHIVE OF MECHANICAL ENGINEERING

Vol. XLIX 2002 Number 1

Key words: *scraping process, scraper's arm, modelling*

TOMASZ PIĄTKOWSKI[*)], *JANUSZ SEMPRUCH*[**)]

SORTING PROCESS OF LOAD UNITS – DYNAMIC MODEL OF SCRAPING PROCESS

The authors present a proposal for modelling the process of scraping of load units (packages) from sorting belt conveyors with the use of deflection scrapers. The continuous scraping process was subjected to discretisation. Characteristic stages of the process were distinguished, such that determine different kinematics-dynamic properties of the load. The created model makes it possible to test the scraping process, and to optimise it.

1. Notations

x, y	–	co-ordinates of the package gravity centre in rectangular system of co-ordinates Oxy,
ϕ	–	angle of load position in relation to conveyor belt,
α	–	scraper's arm deflection angle,
x_o, y_o	–	package gravity centre co-ordinates in rectangular co-ordinate system Ox_oy_o,
F_x, F_y	–	components of resultant friction force F of the package against the conveyor belt,
$\mu_1(v_o), \mu_2(w_x)$	–	friction coefficient,
$L_M=F\,r_T$	–	friction force moment restraining package rotation around its axis,
r	–	radius of instantaneous centre of package rotation,
L_o	–	main friction force moment with r=0,
ξ, η	–	components of relative velocity v_o of the centre C_s with respect to conveyor belt,

*) *University of Technology and Agriculture, Faculty of Telecommunication, Al. Prof. S. Kaliskiego 7, 85-793 Bydgoszcz, Poland; E-mail: topiat@mail.atr.bydgoszcz.pl*

**) *University of Technology and Agriculture, Faculty of Mechanical Engineering, Al. Prof. S. Kaliskiego 7, 85-793 Bydgoszcz, Poland; E-mail: semjan@mail.atr.bydgoszcz.pl*

I, i – package moment and its arm of inertia moment,
m – package mass,
c – package diagonal,
k – restitution coefficient,
r_T – operation arm of resultant friction force,
k_1, k_2 – coefficients dependent on package size,
τ – relative impulse ratio when collision process terminates,
τ_s – relative impulse ratio when slip between bodies terminates or changes its direction,
w_y, w_x – relative velocity of load contact point with the scraper in normal and tangent directions,
M, M_*, K – effective masses.

2. Introduction

Automated sorting systems are applied in large distribution centres. The systems provide a universal solution to all problems connected with sorting and distribution of load units. Thanks to these devices, it is possible to perform the following operations: scraping load units, directing their flow onto transporters, and sort the identified loads onto particular objective lines. The notion of the load unit is very broad. A load unit may be e.g. a large-sized container, a mail package or personal baggage. Because of a great variety of sizes, dimensions, shapes and masses of the loads, in our paper a load unit is assumed to be a mail package whose features are defined in Polish Norm [9], [10]. One of technical solutions used for automatic sorting of load units is the use of sorting machines with scraping devices. These devices are placed along the transporting conveyor, and their working elements could be, for example, pendulously moving arms (Fig. 1).

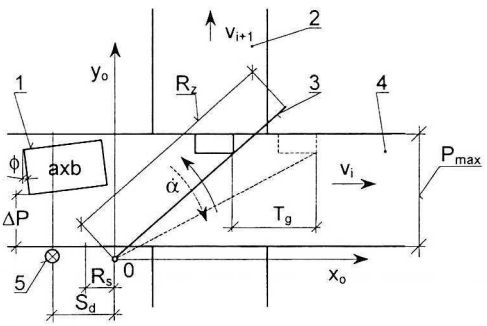

Fig.1. Physical model of scraping process with deflection scraper: 1 – scraped load (dimension axb); 2 i 4 – conveyors; 3 scraper's arm; 5 – light barrier; R_s – position of load front at the moment when scraper's arm begins working; S_d – position of the light barrier; T_g – distance between current position of load and its escaped position; ΔP – distance between load and border of the conveyor; P_{max} – width of conveyor; R_z – length of the scraper's arm; $\dot{\alpha}$ – angular speed; ϕ – angle of load rotation; v_i – linear speed

The presented device characteristics are (because of its simple structure) functionality, long life and reliability that has a great influence on the whole system capacity. One can not control the capacity level arbitrarily, but it must be a matter of conscious choice. A change of one scraping process parameter results in the need to change the other ones. According to technical documentation of the machine [1], its operation requires using such scraping process parameters (conveyor's velocity v, working cycle time of the scraper t_c, position of light barrier S_d, position of the package front during the scraper's reaction R_s) that correspond only with one capacity level of the sorting machine (not the maximal one). Moreover, these parameters do not ensure infallible scraping of all loads allowed for automatic sorting (conclusion drawn from initial tests). However, any parameter changes done by the machine operators during the scraping process are introduced arbitrarily based on the process of tests and errors. The operators do not have sufficient information about the level of the load overloads, which occur while scraping, neither have they knowledge about improper scraping. There is a lack of data necessary for introduction of appropriate changes e.g. concerning the construction that could remove the disadvantages of the scraping process. The solution of this problem may be achieved by creating a dynamic model of scraping process, performing the process simulation and analysing the obtained results.

3. Model of scraping process

Theoretical model of the scraping process was created on the basis of the analysis of different cases of load unit scraping recorded by a video camera during initial experimental tests. The tests were carried out at a research laboratory stand simulating a part of the sorting machine. The permanent scraping process was modelled as a sequence of load motion stages, whose characteristic features occur successively until the load is moved to its destination place. The characteristics result from interaction of loads and working elements of the sorting machine, and indicate these load kinematics-dynamic stages that significantly differ from one another. For this reason, it is necessary to accept an individual mathematical description for modelling the characteristics.

The distinguished discrete stages of the physical scraping process model are:

F1 – oblique strike of the scraper against package corner – the occurrence of the greatest dynamic interactions with the scraped package in the whole scraping process.

F2 – flat motion of the package while rebounding after the strike – slide of the package in relation to the conveyor's belt, when the parcel beyond the conveyor's belt is not in contact with any other element of the machine.

F3 – repeated oblique strike against the scraper (without rebound) – dynamic interaction smaller than during the first strike, when velocity of the pressing belt does not allow for rebound of the load from the scraper.

F4 – rotation of the package around the corner of the rubbing scraper's arm – the package moves on the sorting conveyor belt in flat motion, while one of the package corners remains in permanent contact with the scraper's arm.

F5 – package motion along the scraper's arm – the package side rubs against the scraper's arm and moves on it onto the side of the conveyor opposite to the fixing point of the scraping device.

F6 – scraping the package situated at the closest distance from the axis of rotation (the parcel is not situated on the arm) – the package on the sorting conveyor belt makes a flat movement, and at the same time one of its corners beings moving onto the belt conveyor flight, and another one moves along the scraper's arm.

One can see from the description of the above characteristic stages of the load motion that, in the construction of the scraping process physical model, it is necessary to use basic physical phenomena, such as:

- oblique strike of rough bodies,
- slide dry friction,
- flat motion of package,
- rotary motion of scraper's arm.

In order to facilitate the analysis, some simplifying assumptions have been accepted:

- the parcel is treated as a flat stiff body with evenly distributed mass,
- the contact surfaces of the package with the elements of the sorting machine are non deformable either, which means that neither regular pressure force of the package nor the accompanying friction force can produce elastic deformation or plastic strains in the contact area,
- homogenous frictional properties were assumed all over the entire belt of the conveyor and for the scraped package.
- precession phenomenon was neglected,
- during the scraper's working cycle t_c there is only one package within the working area – the boundary of the scraper reaction area is determined by the position of the light barrier S_d (Fig. 1).

Mathematical model of the scraping process was built on the basis of a physical model of package motion equation with the use of the force balance rule (d'Alambert's rule – F2, F4, F6), II type Lagrange equations (F5), and classic strike theory (F1, F3). Schematic presentation of the distinguished stages characteristic for the package motion and their suggested descriptions is presented in the Appendix [11], [12]. On the basis of the analysis of the selected scraping process stages, one created a numerical model of scraping process in the form of a block diagram (Fig. 2). The sequence of package characteristic stages depends on the way the conditions that decide of the package position on the conveyor's belt are fulfilled. Depending on the package position on the conveyor's belt before scraping, one can realise all stages of the package movement or only some of them. In very few cases (for a particular position of

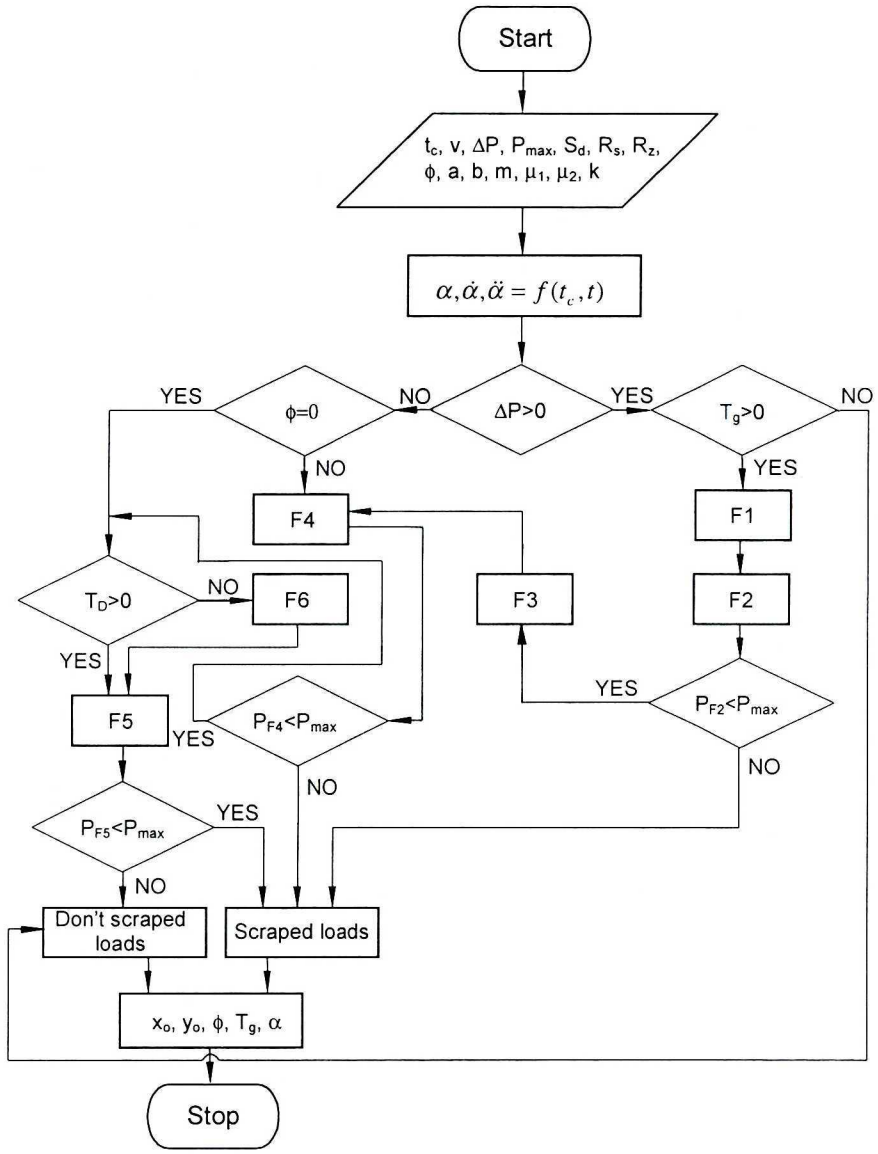

Fig. 2. Diagram of a numeric model: P_{F2}, P_{F4}, P_{F5} – displacement of the load centre of gravity in the direction of axle y_o (in co-ordinates system of Ox_oy_o) reached during realisation characteristic stages F2, F4, F5, T_D – co-ordinate x_o of the load's corner D (table 1)

the package) scraping may occur in one scraping stage – like a slide on the scraper. The list of anticipated cases is as follows:

1) When the package is transported closest to the scraper rotation axis (ΔP=0) and is placed:
   - parallerly to the belt axis (ϕ=0), there follows a slide without striking along the scraper's arm,

- at an arbitrary angle toward the belt axis ($\phi \neq 0$) – there occurs rotation around the corner while touching the scraper until the package is moved along the arm, and then it continues motion along the scraper onto the skid.

2) When the package is at a distance from the scraper axis during transporting ($\Delta P > 0$) and contact between the package and the scraper ($T_g > 0$) is possible:
   - oblique striking of a corner against the scraper, flat movement during rebound, rotation around the corner that rubs the scraper (until the parcel it is positioned parallerly to the arm) and movement along the scraper onto the skid.

The oblique striking of the scraper against the load that occurs during scraping has a decisive influence on the occurrence of overload and the package kinetic characteristics in the scraping process. The striking process characteristic is then the occurrence of reaction forces, which become a source of intensive strain (deformation). The wave spreads all over the volume of colliding bodies, and it reflects several times from limiting surfaces. These processes are accompanied by energy dissipation and shallowing of the strain wave front. In the theoretical approach adopted in this paper, the so-called local effects (local deformations) that occur in the vicinity of the contact point have been distinguished. These effects differ from the reaction of bodies in the points distant from the contact point and pertain to the so-called general deformations. Today it is not possible to talk about existence of any general strike theory, but only discuss the possibility of distinguishing a certain group of dynamic problems, which can be described by means of an equation or a system of equations. Such equations can be solved analytically, or more often, by means of approximate numerical methods. The basis for formulating the dependence of the force in local deformation in the contact problem is given by the theory by H. Hertz, or a more general one, by I. J. Sztajerman [8]. These are basically static theories, however, the results of numerous experiments confirm the possibility of transcribing them on the grounds of dynamics. However, it is possible only to a limited degree, when the dynamic plasticity limit of colliding bodies is not exceeded, and only elastic striking is considered. The contact problem theory is based on the model of quasi-stiff body that, when affected by concentrated external forces, is subjected only to local deformations. Wave effects are neglected (these are general deformations). This theory refers only to bodies of compact structure (i.e. the so-called spherical ones with the exception of the cone cutting edge and the wedge). The other, opposite point of view, consists in considering only wave effects caused by the strikes without taking into consideration any local effects. The first problem of this type, solved by Saint Venant, refers to collinear collision of straight bars with flat front surfaces and transverse striking against a simply-supported bar. Nowadays, both solutions have only historical significance. Oblong striking bars with spherically rounded ends were precisely solved by J. E. Sears, whereas transverse central striking of spherical body against an elastic beam was solved by

S. P. Timoshenko. Although both mentioned problems have a practical significance, they are merely a small fragment of dynamic problems.

The above solutions are not suitable for the use in the case of eccentric collision of bodies on the scraper [6]. The presented problem can be solved in most effective way by means of the so-called restitution energetic coefficient [4] determined experimentally. This coefficient, unlike the Newton's kinematic restitution coefficient, fulfils the rule of energy preservation in the case when direction of slide changes or slide disappears during striking [3], [5]. Unfortunately, in this way one can not determine such quantities as force and length of the strike or the deformation degree. However, in order to compare the dynamic reactions acting on the package during striking against the scraper in the scraping process with limited overloads, such as those the package is subjected to during free fall from the height of 0,3 m onto an undeformable surface [9], it is enough to know the value of the force impulse – which is determinable in the classical striking theory.

In the scraping process, dry sliding friction prevails. Analysis of this phenomenon requires an interdisciplinary approach, [7] as the friction is an effect o a great number of interacting processes. Although friction is easily measurable, it is a complicated phenomenon. Particular difficulties in identifying properties of the friction phenomenon appear at slide velocities close to zero, and that case has a special importance, for example in robotics for precise positioning of link (Dahl's and Streibeck's effect emergency). In the considered model, the velocities of the sliding bodies in scraping process are relatively high, and the influence of the phenomena in the vicinity of zero is not very important. Friction is treated here in a macroscopic scale in which its elementary value $dF=\mu(v_o)dN$ is calculated according to Columb's law ($\mu(v_o)$ – friction coefficient is determined experimentally in the function of velocity for a given frictional pair, dN – elementary normal pressure force).

4. Model analysis

4.1. Package motion paths in the scraping process

While selecting sorting parameters, we have assumed so far that the position of the package front R_s (Fig. 3) at the moment of the scraper's reaction should have a constant value equal to 0,8 m [1] independent of the belt movement velocity v. In the meantime, in the result of the analysis of the scraping process, it turned out that the position R_s has a changeable character, and depends on the velocity v. One needs, however, to obtain the displacement across the belt conveyor flight equal to that recommended by the manufacturer of the sorting machine and in the work [1], and equal to those applied in the sorting machine (t_c=1,36 s, v=0,65 m/s, R_s=0,8 m – Fig. 3) situated at the belt conveyor flight side. The equality must hold for different velocities v, and for the scraper working cycle t_c=1,36 s. For this purpose, it is necessary to set proper delay of

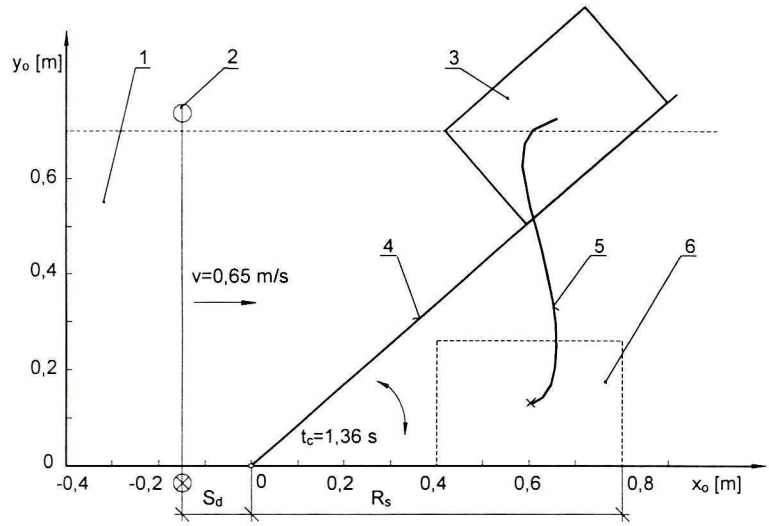

Fig. 3. Path of package that is moved by scraping arm: 1 – separating belt conveyor, 2 – light barrier, 3 – maximum displacement of the package in traverse direction, 4 – scraping arm, 5 – package path, 6 – position of the package when scraping arm starts, scraping data: t_c=1,36 s, v=0,65 m/s, R_s=0,8 m, ΔP=0 m

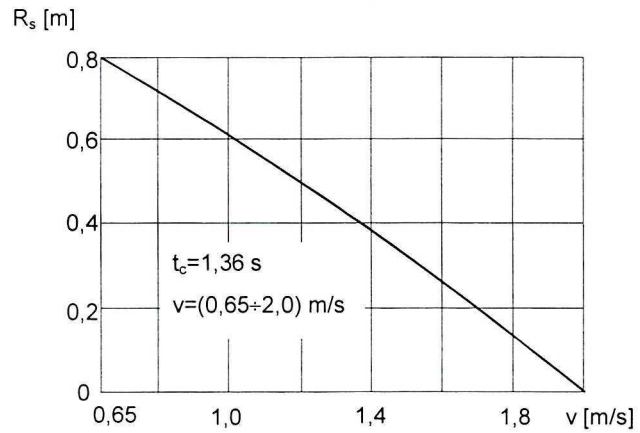

Fig. 4. Lenght of package patch measured from axis of scraper arm up to scraper arm start point R_s (which is equivalent to the same traverse movement of the package), realised discrete stages of the scraping process F5 and F6

scraper's operation start, selecting a proper value of R_s (Fig. 4). As the belt velocity increases, the scraper's reaction must be shortened. For belt velocity v=2 m/s the scraper should start operating when the package is in the position R_s=0 m. It means that by shortening the whole scraping process cycle we achieve a better sorting capacity. Additionally, the increase of the belt velocity and acceleration shortens the scraper's reaction after crossing the light barrier,

and improves the reliability of scraping packages of limiting dimensions (the ones that are allowable to be sorted automatically) in the least favourable situations when:

- a package with the smallest limiting dimensions 0,2×0,1×0,1 m is moved within the longest distance from the scraper axis,
- a package with limiting dimensions 0,7×0,1×0,1 m is moved within the shortest distance from the scraper axis.

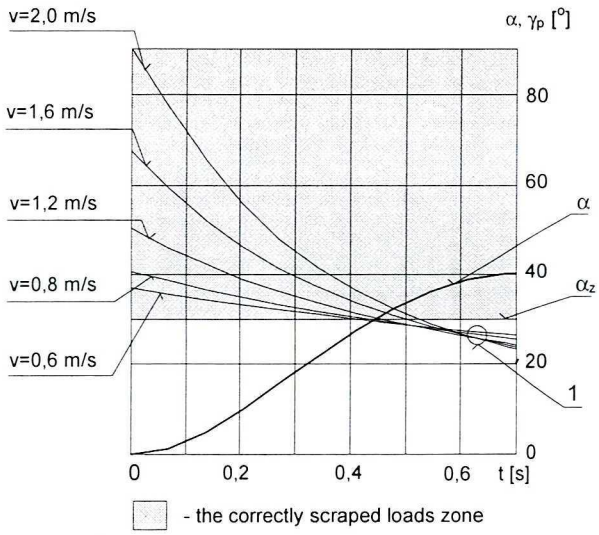

Fig. 5. Diagram of scraper's arm position at the moment of contact with package in function of time t: α – path of scraper's arms, γ_p – path of package's corner

The graph in Fig. 5 a shows whether the scraper would get in touch with the package of limiting dimensions 0,2×0,1×0,1 m in the first case of disadvantageous position of the package on the belt. The scraper working cycle t_c=1,36 s and different velocities v of the belt were assumed. It was also assumed that the package front position R_s at the moment when the scraper starts working depends on velocity v. The scraper strikes against the package when the package front corner path $\gamma_p=f(v, R_s)$ (marked in Fig. 5 as the line 1), intersects the scraper path α above the line α_Z (the package will not „escape" the scraper that is it remains within the scraping area). The analysis of Fig. 5 shows that the higher belt velocity v, the higher the scraper's reliability. The package is stricken not only by scraper's end, but also by the part remote from the end. The scraper's arm path of motion $\alpha(t)$ and its time derivatives were designed for a driving system base on articulated mechanism. Kinetic characteristics of this system were designed with the help of algebraic method that treats the articulated mechanism as a closed polygon of vectors.

A package with limiting dimensions 0,7×0,1×0,1 m that is transported the

closest to the scraper rotation axis can not be scraped (the motion path of the package gravity centre can not to intersect the whole width of the belt conveyor flight – P_{max}=0,7 m) when working parameters are as given by the machine technical documentation (v=0,65 m/s, t_c=1,36 s, R_s=0,8 m – Fig. 6). Only the increase of distance of the package from the conveyor equal to ΔP=0,45 m (Fig. 7), and positioning the parcel parallel to the belt movement direction, allows for placing the package onto the skid while scraping.

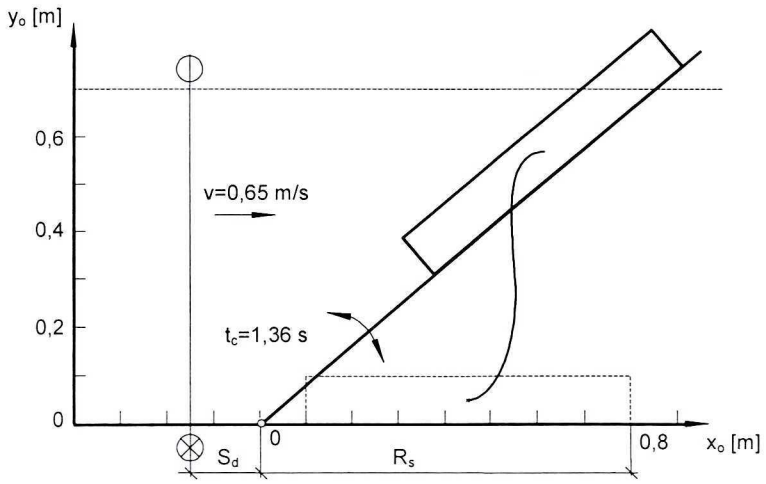

Fig. 6. Path of package that is moved by scraping arm: scraping data: t_c=1,36 s, v=0,65 m/s, R_s=0,8 m, ΔP=0 m

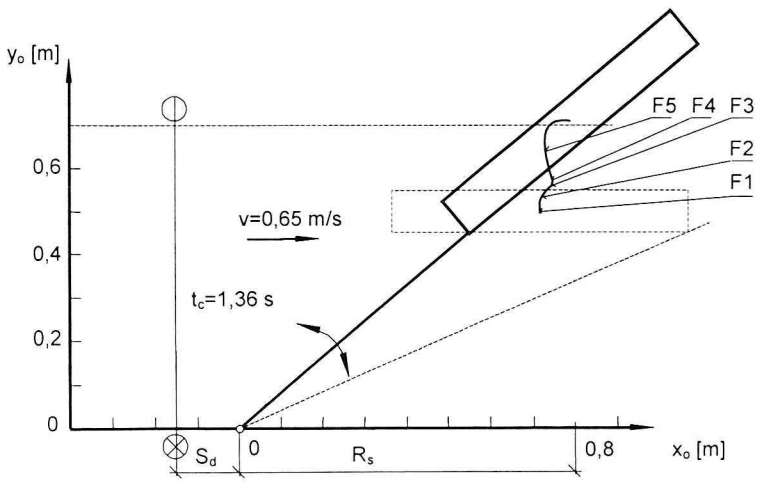

Fig. 7. Path of package that is moved by scraping arm: scraping data: t_c=1,36 s, v=0,65 m/s, R_s=0,8 m, ΔP=0 m; F1, F2, F3, F4, F5 – discrete stages of the scraping process

Placing the package on the belt axis does not guarantee that the package is moved onto the skid. It happens when the package (0,7×0,1×0,1 m) is placed parallel to the scraper before striking. Scraping becomes possible when the parcel is at an even longer distance from the scraper rotation axis. Setting the scraper parameters to t_c=1,36, v=2 m/s, R_s=0 m (Fig. 8) makes it possible to scrape the package towards the skid (the package gravity centre crosses the conveyor's edge).

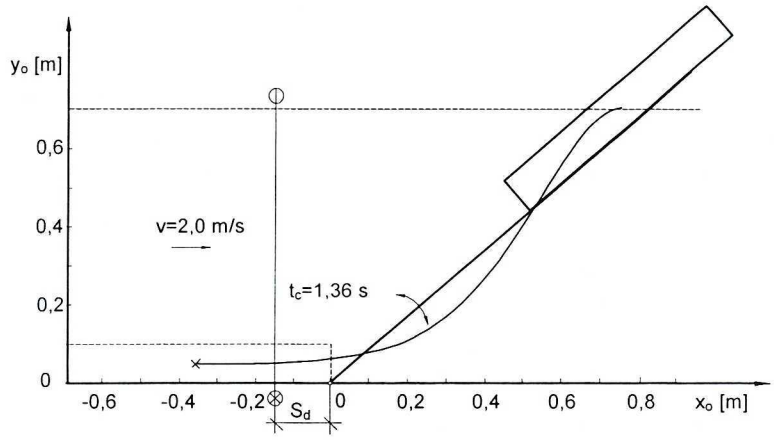

Fig. 8. Path of package that is moved by scraping arm: scraping data: t_c=1,36 s, v=2 m/s, R_s=0 m, ΔP=0 m

4.2. Algorithm of scraper parameters choice

The algorithm was used in order to describe the influence of scraper's parameters (belt velocity v, scraper working cycle t_c, position of light barrier S_d and the value of R_s) on scraping capacity W. The parameters were selected in an interactive way. For each scraper working cycle t_c and belt velocity v, one sought for the value of R_s that would allow for reliable scraping of all packages inserted into the machine. Calculations were performed for limiting overload for a package (that is 15 kg) in the case when the package highest allowable mass was scraped with its striking the scraper in the longest distance from the scraper's arm rotation axis in the moment of its reaching the maximal angular velocity. The spatial record of the results obtained by means of the algorithm is shown in Fig. 9.

4.3. Scraping process optimisation

The quest for optimal scraping process parameters was undertaken on the basis of a numerical optimisation method. In the objective optimisation function, a statistic genetic and deterministic gradient method of the quickest fall with the exterior punishment function was used. The first one confirms

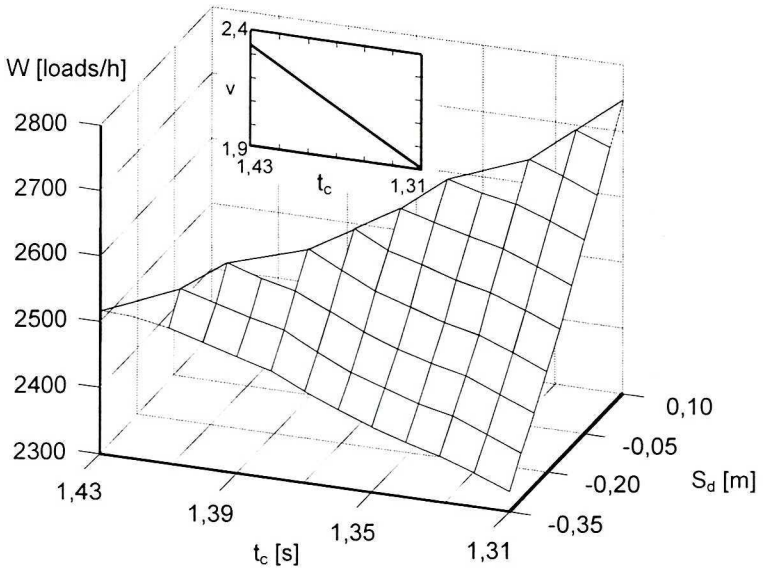

Fig. 9. Sorting capacity as a function of scraper's working cycle t_c and position of the light barrier S_d

globality of the solution of the optimisation task. It leads a directed random search for the optimal point, at the same time not allowing to be stuck in the local extremum. The second method should describe the optimal point more quickly and more precisely, if the existence of local objective function extremes is excluded. Accepting the exterior punishment function in the gradient method enables us to determine a given starting optimisation point not belonging to the allowable solution space.

For the optimised function of task objective one accepted a maximisation of the scraping process capacity. Variables used earlier in the scraping parameter choice algorithm were accepted as decision variables of the scraping process. One has adopted the principle of not exceeding allowable overloads by the package during scraping for the least advantageous scraping conditions as well as the requirement of crossing the opposite conveyors edge by the package gravity centre as limitations restricting the allowable solution space.

Calculations with the use of the above mentioned methods were done three times. In the genetic method, the first attempt to determine the optimal point was made within a wide range: v=(1,0÷2,3) m/s, t_c=(1,0÷1,5) s, R_s=(0÷0,9) m and two other attempts within a more narrow range: v=(1,5÷2,3) m/s, t_c=(1,0÷1,5) s, R_s=(0÷0,5) m. In the quickest falling method the start was made three times at different starting points of decision variables: v=1,8 m/s, t_c=1,5 s, R_s=0,5 m; v=2,1 m/s, t_c=1,2 s, R_s=0,1 m; v=1,9 m/s, t_c=1,1 s, R_s=0 m.

The results obtained by means of numerical optimisation methods (genetic and the fastest falling) are presented in the form of charts (Fig. 10 and 11). In each

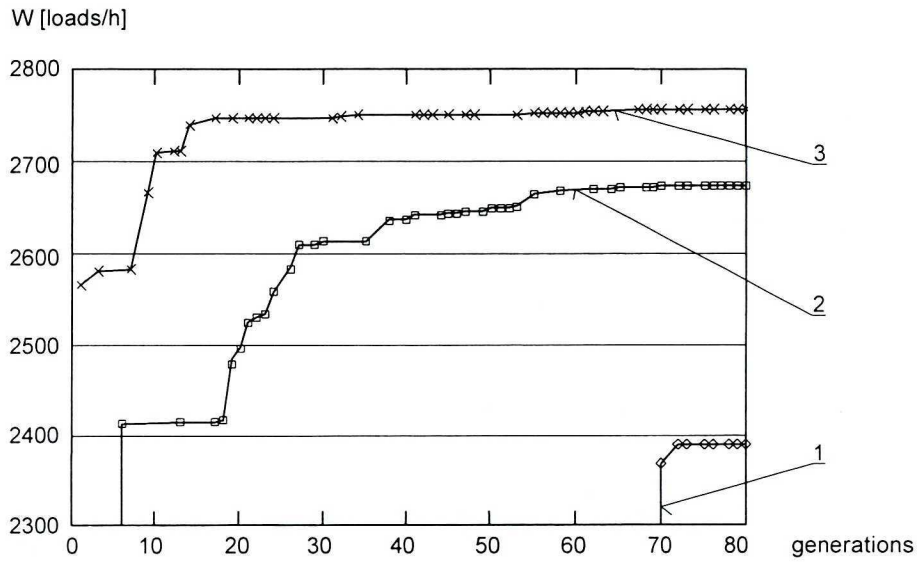

Fig. 10. Results of the scraping process optimisation (genetic method), marked series respond to number of tests: 1) v=(1,0÷2,3) m/s, t_c=(1,0÷1,5) s, R_s=(0÷0,9) m, 2) v=(1,5÷2,3) m/s, t_c=(1,0÷1,5) s, R_s=(0÷0,5) m, 3) v=(1,5÷2,3) m/s, t_c=(1,0÷1,5) s, R_s=0÷0,5m

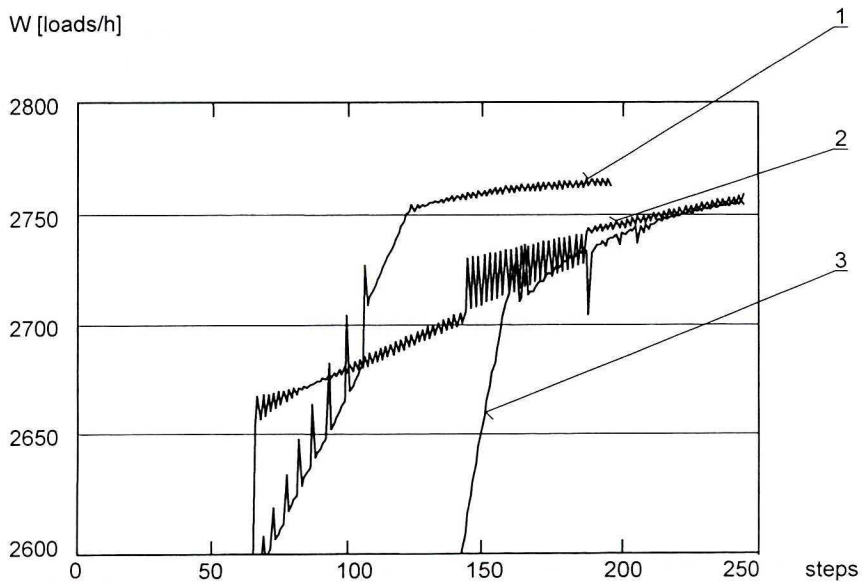

Fig. 11. Results of the scraping process optimisation (gradient method), marked series respond to number of tests: 1) v=1,8 m/s, t_c=1,5 s, R_s=0,50 m, 2) v=2,1 m/s, t_c=1,2 s, R_s=0,10 m, 3) v=1,9 m/s, t_c=1,1 s, R_s=0 m

of them, the results obtained in the three tests are shown. In the case of optimisation of the scraping process parameters by means of the genetic method it turned out that the area of allowable solutions is a „bottle neck" (data series 1, Fig. 10). For 80 generations and 100 populations, decision variables from the allowable solution space were found with the use of the genetic method only 8 times. Optimisation attempts carried out for different limits of decision variables lead to obtaining similar points: $v=(1,91\div1,99)$ m/s, $t_c=(1,30\div1,31)$ s, $R_s=(0,05\div0,10)$ m. The results of the genetic method were supported by the results generated by means of the gradient method for different starting points. The proposed optimal parameters from the available sorting machine sets, are: $v=2$ m/s, $t_c=1,36$ s, $R_s=0$ m, $S_d=0$ m.

5. Experimental tests

5.1. Determining the real motion path of the package

The course of the experiment of package scraping (prepared according to [10]) was registered by a monochromatic video camera CCD K-45R Elemis (with an electronic shutter 1/2000 s) hung above one part of the scraping machine prepared for scraping tests (Fig. 12), and was recorded by a video camera covered with black anti-reflecting paper and with a white sign in the form of a cross placed on it. On the cross, there was a contrasting control point with a diameter equal 2 mm. The recordings of the scraping process were

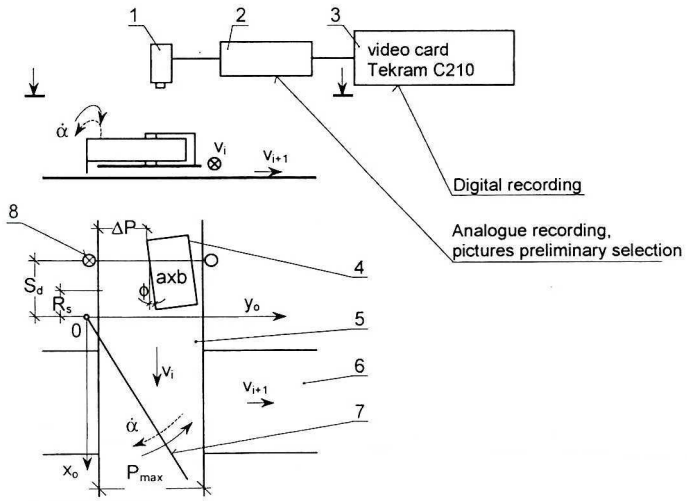

Fig. 12. Recording system of the load path: 1 – camera, 2 – video cassette recorder, 3 – computer, 4 – load (dimension a×b), 5 and 6 – conveyors, 7 – scraper's arm, 8 – light barrier, S_d – position of the light barrier, R_s – position of the load front at the start scraping moment, ΔP – distance of the load from the border of the conveyor, v_i – linear speed, $\dot{\alpha}$ - angle speed, ϕ – angle of the load rotation

watched frame by frame and pictures recorded in the format of bmp files were imported to the graphic editor MS Paint and the position of the marker on the package was read with the accuracy of one pixel. The successive position of the package marker from a particular frame determines the path of motion of the package gravity centre during scraping. The picture was recorded with the resolution of 640×480 points. The distance 0,6 m marked with a ruler on the belt conveyor flight side corresponds with 304 points in the graphical editor's picture.

In Fig. 13 and 14 the package motion paths are drawn near one another in relation to the sorting conveyor frame (in the co-ordinate system Ox_oy_o) – they are obtained by computer simulation (1) and recorded by a video camera (2). Fig. 13 shows the path of motion of gravity centre of the parcel with the dimensions 0,7×0,1×0,1 m when before scraping it was situated near the inner end of the conveyor belt (ΔP=0 m), Fig. 14 – when it was placed in the belt axis. In the case of a package 0,7×0,1×0,1 m situated at the conveyor side, whose belt velocity was low, the obtained compatibility of paths was high (theoretical and real, Fig. 13a) and the consistency was a little smaller when the belt velocity was higher (Fig. 13b). Similar results were obtained during scraping of the package of compact structure (0,4×0,26×0,15 m, Fig. 15) when before scraping it was placed in the belt conveyor axis.

The compatibility was much worse when the scraped package had an oblong shape (0,7×0,1×0,1 m, Fig. 14) and it was also placed in the belt conveyor flight axis. The discrepancy of the package motion paths results from different ways in which there are moved along the conveyor axis.

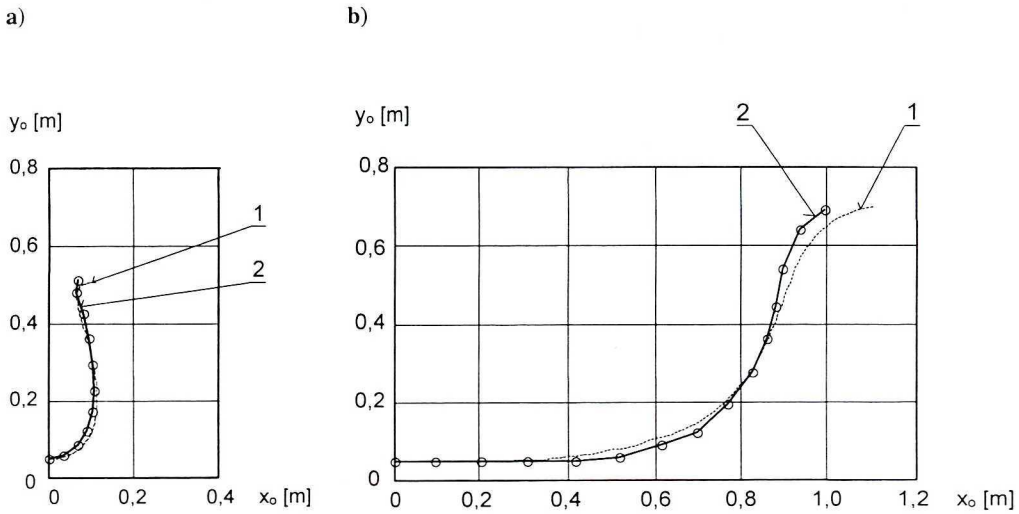

Fig. 13. Path of motion of package gravity centre (0,7×0,1×0,1 m, ΔP=0 m) in relation to the sorting conveyor frame: 1) the model simulation results, 2) recorded by a video camera; scraping parameters: a) t_c=1,36 s, v=0,65 m/s, R_x=0,8 m, b) t_c=1,36 s, v=2 m/s, R_x=0 m

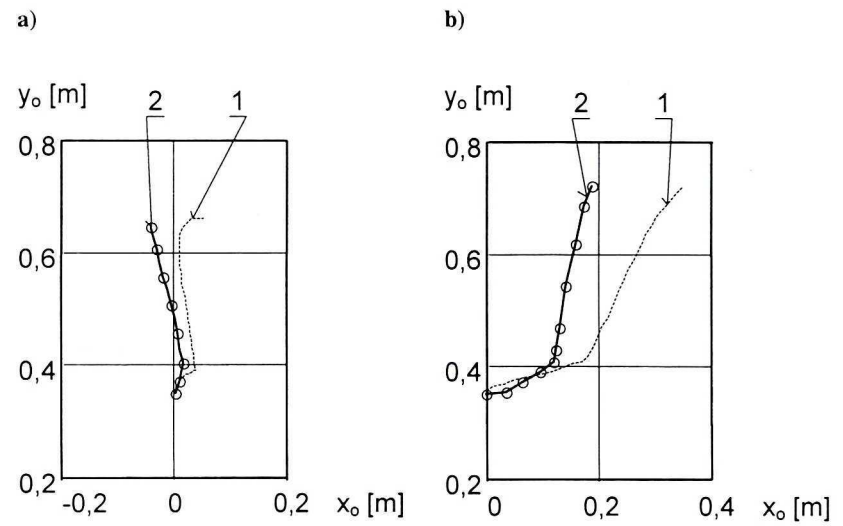

Fig. 14. Path of motion of package gravity centre (0,7×0,1×0,1 m, ΔP=0,3 m) in relation to the sorting conveyor frame: 1) the model simulation results, 2) recorded by a video camera; scraping parameters: a) t_c=1,36 s, v=0,65 m/s, R_s=0,8 m, b) t_c=1,36 s, v=2 m/s, R_s=0 m

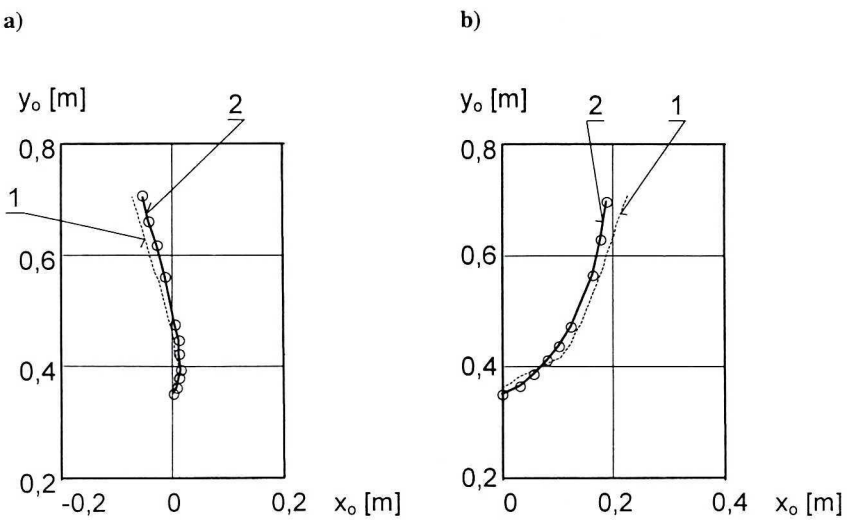

Fig. 15. Path of motion of package gravity centre (0,4×0,26×0,15 m, ΔP=0,22 m) in relation to the sorting conveyor frame: 1) the model simulation result, 2) recorded by a video camera; scraping parameters: a) t_c=1,36 s, v=0,65 m/s, R_s=0,8 m, b) t_c=1,36 s, v=2 m/s, R_s=0 m

However, these discrepancies do not include the model value for evaluating the degree of the package scraping condition fulfilment. The model allows for a proper evaluation of the package displacement in the direction transverse to the belt axis, thus it allows to check the limitation whether, for given parameters of the scraping process, the package will or will not be scraped. The differences in

displacement of the package centre result mainly from the complicated and difficult for modelling nature of friction resistance. Another reason for the package motion path divergences is connected with the package and scraper elastic-dampening properties that are difficult to describe mathematically, and which are represented by the restitution coefficient in the scraping model.

5.2. Experimental testing of package overloads during scraping on sorting machine and in free fall

For evaluating overloads that the package is subjected to during scraping or during its free fall onto an undeformable surface, a specially constructed seismic transformer, equipped with a recording system, was mounted on the package.

Fig. 16 presents the results of experimental tests of the package overloads during scraping on the sorting machine (dispersion bounds 2) and during its free fall (horizontal intermittent lines). It also includes the curve (1) showing the results of theoretical calculations the dynamic reaction between the scraper and the package. The curve is placed in such a way that in Fig. 16 it takes the overload value that corresponds with the height of the free fall H_0=0,2 m and H_0=0,3 m for the same belt velocity v as that obtained by means of mathematical calculations. From the analysis of Fig. 16 one can conclude that during the tests the package overloads were smaller than those determined by mathematical calculations.

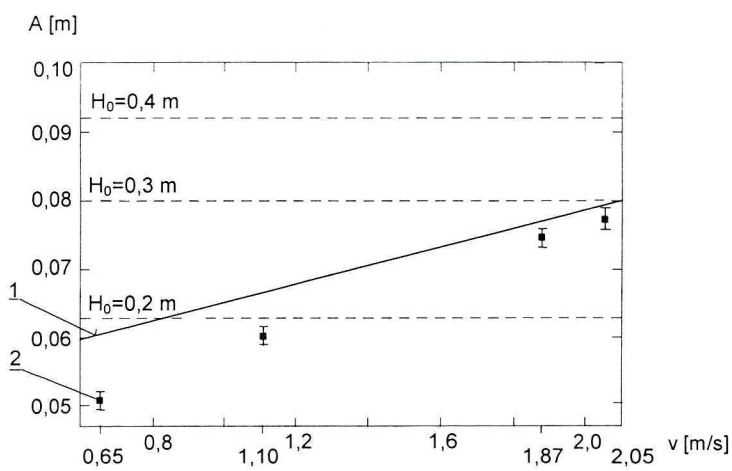

Fig. 16. Overload reached during free fall and scraping of the package in sorting machine for the scraping working cycle t_c=1,36 s: 1- theoretical modelling, 2 – experimental research; A – amplitude of a seismic mass deflection

For low belt velocities the real dynamic effect of the scraper on the parcel differed more significantly from the theoretical one. As the velocity reached v=2 m/s a higher compatibility of results was obtained. The application of the

mathematical evaluation model for calculating package overloads for tested belt velocities does not create any danger that real allowable overloads are exceeded (the ones during the fall from the height H_0=0,3 m [2]). The discrepancy of results remains within safe limits for the package, and it can not be damaged anyway.

6. Conclusion

- The constructed analytic model of scraping process taking into account the limitations of the process meets the expected requirements:
  - experimental tests of the load motion path show that the mathematical model of the scraping process evaluates the displacements of the load across the belt conveyor flight in a proper way i.e. describes properly the characteristic that is used for evaluation of the degree of scraping fulfilment,
  - experimental verification of the gives overloads that appear in the sorting machine during scraping and during a free fall the basis for assuming that the theoretical description of load dynamic reactions during striking against the scraper is proper in to allowable overloads; analytic determination of the overloads may guarantee the respect that real allowable overloads will not be exceeded.
- The differences between the load motion paths (theoretical and real) in the direction of the belt conveyor axis occur while scraping slender loads in the case when during scraping the load strikes against the scraper, especially for higher striking velocities. Displacements of compact structure loads are determined much more precisely.
- The model of scraping process makes it possible to search for parameters that would meet the required restrictions, and at the same time ensure obtaining the assigned or maximum level of sorting capacity, appropriate for the load transporting system in which the sorting machine is employed.

***

APPENDIX

Physical model of the scraping process and basic equations of the mathematical model

F1 – oblique strike of the scraper against package corner

Equations that define parameters of package motion after collision (equations depend on the body inclination) [4]:

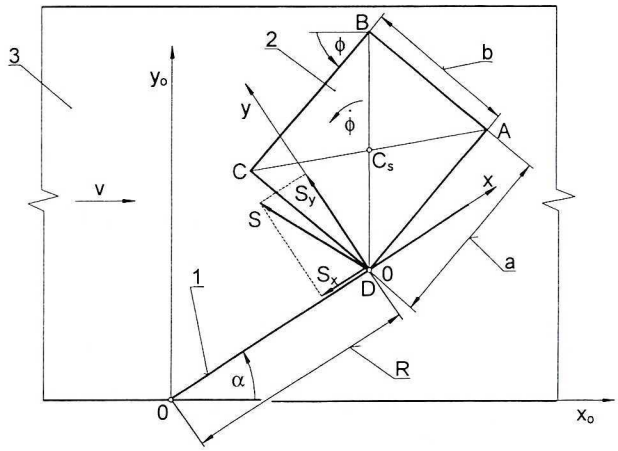

- when slip between bodies doesn't change direction ($\tau_s > 1+k$):

$$\dot{y}(\tau) = w_y(0) + x\dot{\phi}(0) - \frac{w_y(0)M\tau}{m},$$

$$\dot{x}(\tau) = w_x(0) - y\dot{\phi}(0) - \frac{w_y(0)\mu_2(w_x)M\tau}{m},$$

$$\dot{\phi}(\tau) = \dot{\phi}(0) + \frac{w_y(0)\left(x - \mu_2(w_x)y\right)M\tau}{I},$$

$$S = w_y(0)M\sqrt{1+\mu_2(w_x)^2},$$

- when slip between bodies stops or changes slip direction ($0 < \tau_s < 1+k$):

$$\dot{y}(\tau) = w_y(0) + x\dot{\phi}(0) - \frac{w_y(0)}{m}\left[\tau_s M + (\tau - \tau_s)M_*\right],$$

$$\dot{x}(\tau) = w_x(0) - y\dot{\phi}(0) - \frac{w_y(0)\mu_2(w_x)}{m}\left(\tau_s M - (\tau - \tau_s)M_*\right),$$

$$\dot{\phi}(\tau) = \dot{\phi}(0) + \frac{w_y(0)}{I}\left[\tau_s\left(x - \mu_2(w_x)y\right)M + (\tau - \tau_s)\left(x + \mu_2(w_x)y\right)M_*\right],$$

$$S = w_y(0)\left[\tau_s M + (\tau - \tau_s)M_*\right]\sqrt{1+\mu_2(w_x)^2},$$

moreover:

$$\tau_s = \frac{w_x(0)K}{\mu_2(w_x)w_y(0)M},$$

$$\tau = \begin{cases} 1 + k^2\sqrt{(1-\tau_s)^2 + \tau_s(2-\tau_s)\dfrac{M}{M_*}} & \tau_s < 1, \\ \tau = 1 + \sqrt{(\tau_s - 1)^2\left(1 - \dfrac{M}{M_*}\right) + k^2\dfrac{M}{M_*}} & 1 < \tau_s < 1+k, \\ 1+k & 1+k < \tau, \end{cases}$$

$$M = I\left(i^2 + x^2 - \mu_2(w_x)xy\right)^{-1},$$

$$M_* = I\left(i^2 + x^2 + \mu_2(w_x)xy\right)^{-1},$$

$$K = I\left(i^2 + y^2 - \frac{xy}{\mu_2(w_x)}\right)^{-1},$$

$$w_x(0) = v\cos\alpha,$$

$$w_y(0) = R\dot{\alpha} + v\sin\alpha.$$

F2 – flat motion of the package

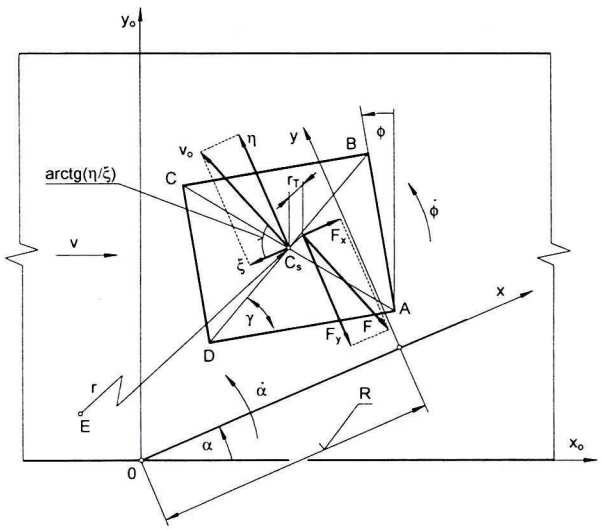

System of equations of force and moment balance:

$$\begin{cases} m\ddot{x} = F_x \\ m\ddot{y} = -F_y \\ I\ddot{\phi} = -L_M \end{cases},$$

moreover [13]:

$$F_x = mg\mu_1(v_o)tgh\left(\frac{k_1}{\dot{\phi}}v_o\right)\cos\left(arctg\frac{\eta}{\xi}\right),$$

$$F_y = mg\mu_1(v_o)tgh\left(\frac{k_1}{\dot{\phi}}v_o\right)\sin\left(arctg\frac{\eta}{\xi}\right),$$

$$L_M = Lo\exp\left(-\frac{k_2}{\dot{\phi}}v_o\right) + mg\mu_1(v_o)\frac{1}{\dot{\phi}}v_o\left[1 - tgh\left(\frac{k_1}{\dot{\phi}}v_o\right)\right],$$

where:

$$\xi = v\cos\phi - \dot{x},$$

$$\eta = v\sin\phi + \dot{y}.$$

F3 – repeated oblique strike against the scraper (without rebound) – description of the step F1

F4 – rotation of the package around the corner of the rubbing scraper's arm

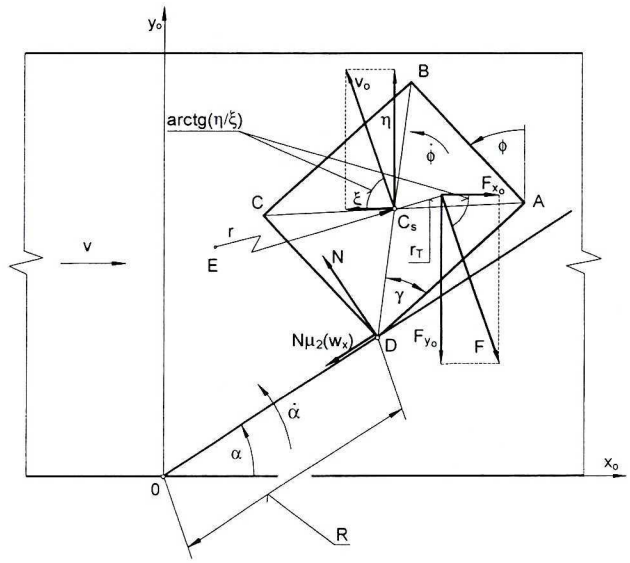

System of equations of force and moment balance:

$$\begin{cases} m\ddot{x}_o = F_{x_o} - N\left(\mu_2(w_x)sign(w_x)\cos\alpha + \sin\alpha\right), \\ m\ddot{y}_o = -F_{y_o} + N\left(\cos\alpha - \mu_2(w_x)sign(w_x)\sin\alpha\right), \\ I\ddot{\phi} = -\frac{c}{2}N\left[\cos(\gamma-\alpha+\phi) + \mu_2(w_x)sign(w_x)\sin(\gamma-\alpha+\phi)\right] - L_M. \end{cases}$$

System of equations has three equations and four unknowns – $x_o(t)$, $y_o(t)$, $\phi(t)$, $N(t)$. The fourth missing equation may be assigned by double differentiation of the dependency describing the co-ordinate of the package gravity centre x_o:

$$x_o = \left[P - \frac{c}{2}\sin(\gamma+\phi)\right]ctg\alpha + \frac{c}{2}\cos(\gamma+\phi),$$

moreover:

$$\xi = v - \dot{x}_o,$$

$$\eta = \dot{y}_o,$$

$$w_x = \dot{y}_o\sin\alpha + \dot{x}_o\cos\alpha + \frac{c}{2}\dot{\phi}\sin(\gamma-\alpha+\phi).$$

F5 – package motion along the scraper's arm

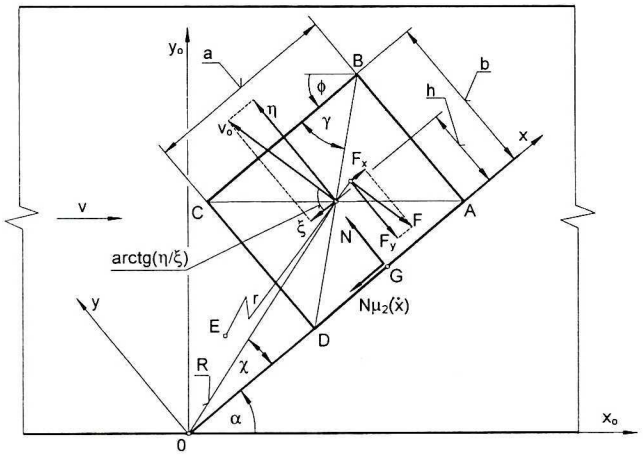

Kinetic energy of the load (two degrees of freedom):

$$E_k = \frac{1}{2} m\left[\dot{x}^2 + \left(R^2 + i^2\right)\dot{\alpha}^2\right].$$

Components of Lagrange equations:

- for co-ordinate x:

$$\begin{cases} \dfrac{\partial E_k}{\partial x} = mx\dot{\alpha}^2, \quad \dfrac{\partial E_k}{\partial \dot{x}} = m\dot{x}, \quad \dfrac{d}{dt}\left(\dfrac{\partial E_k}{\partial \dot{x}}\right) = m\ddot{x}, \\ Q_x = F_x - N\mu_2(\dot{x})sign(\dot{x}), \end{cases}$$

- for co-ordinate α:

$$\begin{cases} \dfrac{\partial E_k}{\partial \alpha} = 0, \quad \dfrac{\partial E_k}{\partial \dot{\alpha}} = m\left(x^2 + h^2 + i^2\right)\dot{\alpha}, \\ \dfrac{d}{dt}\left(\dfrac{\partial E_k}{\partial \dot{\alpha}}\right) = 2mx\dot{x}\dot{\alpha} + m\left(x^2 + h^2 + i^2\right)\ddot{\alpha}, \quad Q_\alpha = (N - F_y)x. \end{cases}$$

Ordered components of Lagrange equations:

$$\ddot{x} = x\dot{\alpha}^2 - \mu_2(\dot{x})sign(\dot{x})\left[2\dot{x}\dot{\alpha} + \ddot{\alpha}\left(x + \frac{h^2 + i^2}{x}\right)\right] + g\mu_1(v_o)th\left(\frac{k_1}{\dot{\alpha}}v_o\right)\left(\xi - \mu_2(\dot{x})sign(\dot{x})\eta\right)\frac{1}{v_o},$$

moreover:

$$\xi = v\cos\alpha + \dot{\alpha}\ R\sin\chi - \dot{x},$$

$$\eta = v\sin\alpha + \dot{\alpha}\ R\cos\chi.$$

F6 – scraping the package situated at the closest distance from the axis of rotation

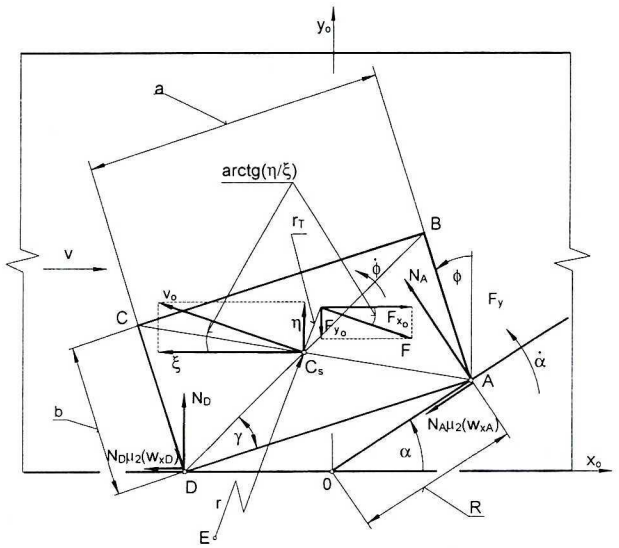

System of equations of force and moment balance:

$$\begin{cases} m\ddot{x}_o = F_{x_o} - N_A\left(\mu_2(w_{xA})sign(w_{xA})\cos\alpha + \sin\alpha\right) - N_D\mu_2(w_{xD})sign(w_{xD}), \\ m\ddot{y}_o = -F_{y_o} - N_A\left(\mu_2(w_{xA})sign(w_{xA})\sin\alpha - \cos\alpha\right) + N_D, \\ I\ddot{\phi} = \frac{c}{2}N_A\left[\cos(\alpha+\gamma-\phi) - \mu_2(w_{xA})sign(w_{xA})\sin(\alpha+\gamma-\phi)\right] - \\ \quad -\frac{c}{2}N_D\left[\cos(\gamma+\phi) + \mu_2(w_{xD})sign(w_{xD})\sin(\gamma+\phi)\right] - L_M. \end{cases}$$

System of equations has three equations and five unknowns – $x_o(t)$, $y_o(t)$, $\phi(t)$, $N_A(t)$, $N_D(t)$. Two missing equations may be assigned by double differentiation of dependency describing the co-ordinates of the package gravity centre x_o and y_o:

$$x_o = a\frac{\sin\phi}{\sin\alpha}\cos\alpha - \frac{c}{2}\cos(\gamma-\phi),$$

$$y_o = \frac{c}{2}\cos(\gamma+\phi),$$

moreover:

$$\eta = \dot{y}_o,$$

$$\xi = v - \dot{x}_o,$$

$$w_{xA} = \dot{y}_o\sin\alpha + \dot{x}_o\cos\alpha + \frac{c}{2}\dot{\phi}\sin(\alpha+\gamma-\phi),$$

$$w_{xD} = \dot{x}_o + \frac{c}{2}\dot{\phi}\sin(\gamma+\phi).$$

Manuscript received by Editorial Board, March 16, 2001;
final version, February 15, 2002.

REFERENCES

[1] Wiatr R., Rawłuszko J.: The parcel sorting machine efficiency analysis and/or sorting reliability enlarging. Science Book ATR (PL), No 169, Bydgoszcz 1990.

[2] Information about permit to postal turn of the postal parcel in typical containers. Technique and Post Exploitation (PL) 4'93.

[3] Brach R. M. Rigid bodies collisions. ASME Journal of Applied Mechanics, Vol. 56, 1989, pp. 133÷138.

[4] Stronge W. J.: Unravelling paradoxical theories for rigid body collisions. ASME Journal of Applied Mechanics, Vol. 58, 1991, pp. 1049÷1055.

[5] Charles E.: Predicting rebounds using rigid-body dynamics. ASME Journal of Applied Mechanics, Vol.58, 1991, pp. 754÷758.

[6] Thornton C.: Coefficient of restitution for collinear collisions of elastic-perfectly-plastic spheres. ASME Journal of Applied Mechanics, Vol.64 1997, pp. 383÷386.

[7] Lotstedt P.: Coulomb friction in two-dimensional rigid body systems. Zeitschrift fur Angewandte Mathematic und Mechanic, Vol.61 No.12, 1981, pp. 605÷615.

[8] Gryboś R.: Collisions theory in discrete mechanical systems. PWN, Warszawa 1969.

[9] PN–92/O–79100/02, Complete filled transport packages, Quantitative data, (PL).

[10] PN–98/T–85000, Typical containers for postal parcels, (PL).

[11] Piątkowski T., Sempruch J.: Model and analysis of selected features of scraping process. Tenth World Congress on the Theory of Machines and Mechanisms, Oulu 1999.

[12] Piątkowski T.: Analysis of scraping process for example of package separating machine, doctoral dissertation, Bydgoszcz 1999.

[13] Krivoplas A.: Sorting machines. Machine Building, Moskow 1980.

Proces sortowania ładunków jednostkowych – dynamiczny model procesu zgarniania

Streszczenie

Artykuł przedstawia propozycję modelowania procesu zgarniania ładunków jednostkowych (paczek) przy użyciu zgarniaków wychyłowych z taśmowych przenośników rozdzielczych. Ciągły proces zgarniania poddano dyskretyzacji, wyodrębniono z niego stany charakterystyczne, które wyznaczają różne właściwości kinematyczno-dynamiczne ładunku w jakich może się on znaleźć podczas zgarniana. Utworzony model pozwala na badanie i optymalizację procesu zgarniania.